IEEE Access
Multidisciplinary | Rapid Review | Open Access Journal

Received August 21, 2017, accepted September 26, 2017, date of publication October 3, 2017, date of current version October 25, 2017.

Digital Object Identifier 10.1109/ACCESS.2017.2758523

Dynamic Modeling of Networks, Microgrids, and Renewable Sources in the dq0 Reference Frame: A Survey

DMITRY BAIMEL[1], JURI BELIKOV[2], JOSEP M. GUERRERO[3], (Fellow, IEEE), AND YOASH LEVRON[4], (Member, IEEE)

[1]Shamoon College of Engineering, Beer-Sheva 84100, Israel
[2]Department of Computer Systems, Tallinn University of Technology, 19086 Tallinn, Estonia
[3]Department of Energy Technology, Aalborg University, 9220 Aalborg, Denmark
[4]Andrew and Erna Viterbi Faculty of Electrical Engineering, Technion—Israel Institute of Technology, Haifa 3200003, Israel

Corresponding author: Yoash Levron (yoashl@ee.technion.ac.il)

The work of J. Belikov was supported in part by the Grand Technion Energy Program, in part by the Technion Fellowship, and in part by the Estonian Research Council under Grant MOBTP36. The work of Y. Levron was supported in part by the Grand Technion Energy Program and in part by the Technion Fellowship.

ABSTRACT With increasing the penetration of distributed and renewable sources into power grids, and with increasing the use of power electronics-based devices, the dynamic behavior of large-scale power systems is becoming increasingly complex. These recent developments have led to several models attempting to simplify the analysis of dynamic phenomena, among them are models based on the dq0 transformation. Many recent works present dq0-based models of various power system components, ranging from small renewable sources to complete networks. The purpose of this paper is to review and categorize these works, with an objective to promote a straightforward modeling and the analysis of complex systems, based on dq0 quantities. This paper opens by recalling basic concepts of the dq0 transformation and dq0-based models. We then review several recent works related to dq0 modeling and analysis, considering the models of passive components, complete passive networks, synchronous machines, wind turbine systems, photovoltaic inverters, and others.

INDEX TERMS Power systems, microgrids, renewable energy sources.

I. INTRODUCTION

For many years the dynamic behavior of power grids was dictated by large synchronous machines with high inertia and slow dynamic responses. As a result, dynamic processes in interconnected and large-scale power systems were successfully analyzed based on time-varying phasor models (quasi-static models) [1]. A key assumption of time-varying phasor models is that phasors are slowly changing in comparison to the system frequency [2], [3], and therefore AC quantities are mapped to quasi-constant signals. A key advantage of this approach is that the resulting models are time-invariant, and have a well-defined operating point. Due to these properties, quasi-static models have been used extensively in the analysis of dynamic interactions that occur in time frames of seconds to minutes, and have historically enabled studies of machines stability, inter-area oscillation, and other slow dynamic phenomena [4]–[7].

However, in recent years, the increasing penetration of small distributed generators and fast power electronics based devices creates new challenges, one of which is that the system is in many cases not quasi-static. Due to these emerging technologies, voltage and current signals may contain high harmonic components, and can exhibit fast amplitude and phase variations [2]. These developments have led to several alternative models attempting to bridge this gap, among them are models based on the *dq*0 transformation. Such models combine two properties of interest: similar to time-varying phasor models, *dq*0-based models map AC signals to quasi-constant signals, so the resulting model is often time-invariant, with a well-defined operating-point. In addition, *dq*0 models are inherently transient models, and are derived directly from physical representations. As a result, *dq*0-based models do not rely on the assumption of a quasi-static system, and remain accurate at high frequencies [8]. The relations

TABLE 1. Comparison of approaches for dynamic modeling.

model	operating point	small-signal	high frequencies	nonsymmetric networks
time-varying phasors	✓	✓	X	X
abc	X	X	✓	✓
*dq*0	✓	✓	✓	X
dynamic phasors	✓	✓	see text	see text

between different types of dynamic models are presented in Table 1.

Due to these trends, many recent works present *dq*0-based models of various power system components, ranging from small renewable sources to complete networks [9]. The purpose of this paper is to review and categorize these works, with an objective to promote a straightforward modeling and analysis of complex systems, based on *dq*0 quantities. The paper opens by recalling basic concepts of the *dq*0 transformation and *dq*0-based models. We then review several recent works related to *dq*0 modeling and analysis, considering models of passive components, complete passive networks, synchronous machines, wind turbine systems, photovoltaic inverters, and others. We hope that the paper may be a step toward a general dynamic model of large-scale power systems, based on *dq*0 quantities. This in turn may allow a better understanding of the complex dynamics associated with the integration of distributed and renewable sources.

II. OVERVIEW OF DIFFERENT MODELING TECHNIQUES

Several approaches exist for modeling the dynamic behavior of three-phase power systems. One technique is to model the system in the time domain, using the native *abc* reference frame. This approach is often the most general, since it applies, for instance, to non-symmetric or unbalanced systems, and is valid over a wide range of frequencies. Another popular approach is to model the power system using time-varying phasors, often by means of the network power flow equations. This approach has many benefits, one of them is that the network is described using purely algebraic equations. However, time-varying phasors are only applicable at low frequencies, under the assumption that the system is quasi-static. A solution that complements these two well-known approaches is to model power systems on the basis of *dq*0 quantities. This approach is not as general as *abc*-based models, and is advantageous mainly when the network and units are symmetrically configured,[1] see [8] and brief discussion in Section III-B for more details.

[1]By definition, symmetrically configured networks produce symmetric three-phase currents, if fed by symmetric three-phase voltages. For instance, a transmission network with identical circuit in each of the three-phases is symmetrically configured.

Another popular modeling technique is dynamic phasors. Dynamic phasors generalize the idea of quasi-static phasors, and represent voltage and current signals by Fourier series expansions in which the harmonic components are evaluated over a moving time window [10], [11]. The idea behind the dynamic phasors approach is therefore to approximate the system with nearly periodic quantities, which allow an accurate representation of the system while using a relatively large numerical step size [12], [13]. A comparison of simulation techniques based on dynamic phasors in the *abc* and *dq*0 reference frames may be found in [14] and [15], a comparison of several dynamic phasors based models of large-scale networks is presented in [16]. In addition, dynamic phasors have the advantage of efficiently simulating harmonic components, which is not possible with *dq*0-based models. Dynamic phasors have been demonstrated with many system components, including synchronous and induction machines [11], [17], HVDC systems [12], [18], [19], FACTS devices [3], sub-synchronous resonance [20], asymmetric systems [11], [21], and asymmetric faults [17], [22]. In addition, dynamic phasors are utilized in state estimation [23]–[25], in systems with varying frequencies [26], and also in microgrids [27].

III. MODELING AND ANALYSIS OF POWER SYSTEMS BASED ON DQ0 QUANTITIES

We now recall the basic definition of the *dq*0 transformation. Consider a reference frame rotating with an angle of $\theta(t)$. For instance, in a synchronous machine, $\theta(t)$ is typically selected to be the rotor electrical angle. Let $\tilde{x}$ represent the quantity to be transformed (current, voltage, or flux), and use the compact notation $x_{abc} = [x_a, x_b, x_c]^{\mathsf{T}}$, $x_{dq0} = [x_d, x_q, x_0]^{\mathsf{T}}$. The *dq*0 transformation with respect to the reference frame rotating with the angle θ can be defined as [28, Appendix C]

$$\tilde{x}_{dq0} = T_\theta x_{abc} \tag{1}$$

with

$$T_\theta = \frac{2}{3}\begin{bmatrix} \cos(\theta) & \cos\left(\theta - \frac{2\pi}{3}\right) & \cos\left(\theta + \frac{2\pi}{3}\right) \\ -\sin(\theta) & -\sin\left(\theta - \frac{2\pi}{3}\right) & -\sin\left(\theta + \frac{2\pi}{3}\right) \\ \frac{1}{2} & \frac{1}{2} & \frac{1}{2} \end{bmatrix}. \tag{2}$$

Note that there are several variants of the transformation (2) available in the literature; however, all of them are equivalent up to the proper selection of the angle θ and order of the rows [6], [9]. The same applies to the *balanced* (without zero component) version of T_θ known as Park's transformation [29, Appendix A], which was first introduced in [30].

A fundamental property of the *dq*0 transformation is that it maps symmetric AC signals to constants. For instance,

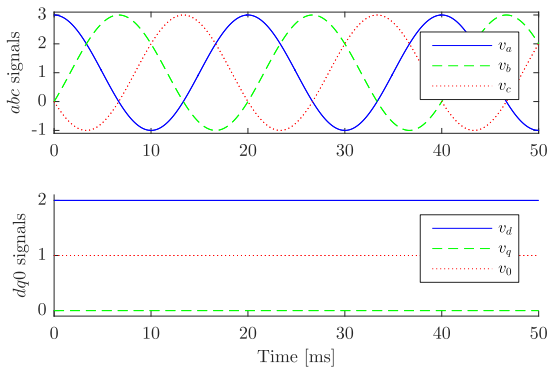

FIGURE 1. An example showing mapping of *abc* signals to *dq0* signals.

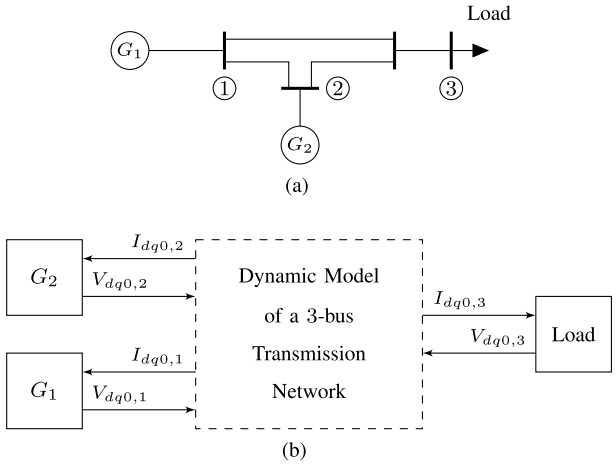

FIGURE 2. Example: *dq0*-based model of a symmetric 3-bus system. (a) Single-line diagram. (b) Signal-flow diagram.

consider the signals

$$\begin{aligned} v_a &= A\cos(\theta) + B, \\ v_b &= A\cos\left(\theta - \frac{2\pi}{3}\right) + B, \\ v_c &= A\cos\left(\theta + \frac{2\pi}{3}\right) + B. \end{aligned} \tag{3}$$

Using the inverse transformation T_θ^{-1}, it is easy to see that

$$\begin{bmatrix} v_a \\ v_b \\ v_c \end{bmatrix} = \begin{bmatrix} \cos(\theta) & -\sin(\theta) & 1 \\ \cos\left(\theta - \frac{2\pi}{3}\right) & -\sin\left(\theta - \frac{2\pi}{3}\right) & 1 \\ \cos\left(\theta + \frac{2\pi}{3}\right) & -\sin\left(\theta + \frac{2\pi}{3}\right) & 1 \end{bmatrix} \begin{bmatrix} A \\ 0 \\ B \end{bmatrix}, \tag{4}$$

and therefore $v_d = A$, $v_q = 0$, $v_0 = B$, see Fig. 1.

When describing complex systems, models based on $dq0$ signals may be presented as signal-flow diagrams, in which each component is modeled by $dq0$ quantities. A simple motivating example is presented in Fig. 2. A question that often appears when modeling systems based on $dq0$ quantities is how to choose the reference frame, or in other words, how to link machines that rotate at different frequencies. One approach presented in [2] and [31] is to model the network and its components using a $dq0$ transformation that is based on a unified (global or common) reference frame, rotating with a fixed frequency ω_s. The frequency ω_s is chosen as follows: if there is an infinite bus in the system, ω_s is selected as the frequency of the infinite bus. If no generator is large enough to be modeled as an infinite bus, then ω_s is equal to the steady-state system frequency. In this case $dq0$ signals will be constant at steady-state, and the system will have well-defined equilibrium point [32].

A $dq0$ transformation based on ω_s is similar to (2), and is obtained by substituting $\theta = \omega_s t = 2\pi f_s t$:

$$x_{dq0} = T_{\omega_s} x_{abc} \tag{5}$$

with

$$T_{\omega_s} = \frac{2}{3} \times \begin{bmatrix} \cos(\omega_s t) & \cos\left(\omega_s t - \frac{2\pi}{3}\right) & \cos\left(\omega_s t + \frac{2\pi}{3}\right) \\ -\sin(\omega_s t) & -\sin\left(\omega_s t - \frac{2\pi}{3}\right) & -\sin\left(\omega_s t + \frac{2\pi}{3}\right) \\ \frac{1}{2} & \frac{1}{2} & \frac{1}{2} \end{bmatrix} \tag{6}$$

A formula that allows to convert signals from the θ reference frame to the unified frame can be derived following [31] as

$$\begin{bmatrix} x_d \\ x_q \\ x_0 \end{bmatrix} = \begin{bmatrix} \sin(\delta) & \cos(\delta) & 0 \\ -\cos(\delta) & \sin(\delta) & 0 \\ 0 & 0 & 1 \end{bmatrix} \begin{bmatrix} \tilde{x}_d \\ \tilde{x}_q \\ x_0 \end{bmatrix}, \tag{7}$$

where $\delta(t) = \theta(t) - \omega_s t + \pi/2$. The variables x_d, x_q are defined with respect to $\omega_s t$, and $\tilde{x}_d, \tilde{x}_q$ are defined with respect to θ.

The total instantaneous three-phase power $P_{3\phi}$ flowing from a unit into the network can be computed as

$$\begin{aligned} P_{3\phi} &= v_a i_a + v_b i_b + v_c i_c = V_{abc}^{\mathsf{T}} I_{abc} \\ &= \left(T_{\omega_s}^{-1} V_{dq0}\right)^{\mathsf{T}} T_{\omega_s}^{-1} I_{dq0} \\ &= \left(V_{dq0}\right)^{\mathsf{T}} \left(T_{\omega_s}^{-1}\right)^{\mathsf{T}} T_{\omega_s}^{-1} I_{dq0} \\ &= \begin{bmatrix} v_d & v_q & v_0 \end{bmatrix} \begin{bmatrix} 3/2 & 0 & 0 \\ 0 & 3/2 & 0 \\ 0 & 0 & 3 \end{bmatrix} \begin{bmatrix} i_d \\ i_q \\ i_0 \end{bmatrix} \\ &= \frac{3}{2}\left(v_d i_d + v_q i_q + 2 v_0 i_0\right). \end{aligned} \tag{8}$$

A. LINEAR PASSIVE COMPONENTS

This section overviews $dq0$ models of linear passive elements [33]–[35]. Such elements form the basis for modeling a large variety of more complex components. We open this discussion by demonstrating the dynamic model of a symmetric three-phase inductor. The inductor model in the native

abc reference frame is given by

$$L\frac{\mathrm{d}}{\mathrm{d}t}I_{abc,12} = V_{abc,1} - V_{abc,2}, \tag{9}$$

and can be converted to the *dq*0 frame as follows. Observe that differentiation of (5) results in

$$\frac{\mathrm{d}}{\mathrm{d}t}I_{dq0} = \frac{\mathrm{d}T_{\omega_s}}{\mathrm{d}t}I_{abc} + T_{\omega_s}\frac{\mathrm{d}}{\mathrm{d}t}I_{abc}, \tag{10}$$

which after simple algebraic manipulations yields

$$\frac{\mathrm{d}}{\mathrm{d}t}I_{dq0,12} = \mathcal{W}I_{dq0,1} + \frac{1}{L}\left(V_{dq0,1} - V_{dq0,2}\right), \tag{11}$$

where

$$\mathcal{W} = \begin{bmatrix} 0 & \omega_s & 0 \\ -\omega_s & 0 & 0 \\ 0 & 0 & 0 \end{bmatrix}. \tag{12}$$

This equation describes a state-space model of a symmetric three-phase inductor. Similarly, the model of a symmetric three-phase capacitor C is given as

$$\frac{\mathrm{d}}{\mathrm{d}t}\left(V_{dq0,1} - V_{dq0,2}\right) = \mathcal{W}\left(V_{dq0,1} - V_{dq0,2}\right) + \frac{1}{C}I_{dq0,12}. \tag{13}$$

And for a symmetric three-phase resistor R the model is given by the simple static relations

$$V_{dq0} = I_3 R I_{dq0}, \tag{14}$$

where I_3 denotes the 3×3 identity matrix.

Now consider briefly how energy is expressed in *dq*0 coordinates. Assume a symmetrically configured three-phase inductor (9). By definition, the stored energy is

$$E = \frac{1}{2}L\left(i_a^2 + i_b^2 + i_c^2\right), \tag{15}$$

which can be rewritten as

$$\begin{aligned} E &= \frac{1}{2}LI_{abc}^{\mathsf{T}}I_{abc} \\ &= \frac{1}{2}L\left(T_{\omega_s}^{-1}I_{dq0}\right)^{\mathsf{T}}T_{\omega_s}^{-1}I_{dq0} \\ &= \frac{1}{2}L\begin{bmatrix} i_d & i_q & i_0 \end{bmatrix}\begin{bmatrix} 3/2 & 0 & 0 \\ 0 & 3/2 & 0 \\ 0 & 0 & 3 \end{bmatrix}\begin{bmatrix} i_d \\ i_q \\ i_0 \end{bmatrix} \\ &= \frac{3}{4}L\left(i_d^2 + i_q^2 + 2i_0^2\right). \end{aligned} \tag{16}$$

B. MODELING SYMMETRIC TRANSMISSION NETWORKS AND MICROGRIDS

By combining models of elementary passive components, any symmetric transmission network can be modeled based on the *dq*0 reference frame. With various degree of details, this problem was addressed in several works. The following cases of transmission/distribution networks have been studied:

- *RL*: the network and loads are modeled in a common *dq* reference frame [31] under the assumption of balanced signals [2], [36]. In [9] this assumption is replaced by a less restrictive assumption, requiring the transmission network to be symmetrically configured.
- *RL with shunt elements and transformers*: a non-minimal state-space model is developed in [37]. Continuing this research, the minimal (controllable and observable) state-space model for the large-scale transmission networks is presented in [38]. This model extends the above models relying on a more general topology as defined in [39] and illustrated in Fig. 4.
- *Microgrids*: particular examples of small microgrids with few buses and several synchronous/distributed generators are presented in [40]–[43]. In [44] a time-domain model for the small-signal analysis of unbalanced microgrids is developed.

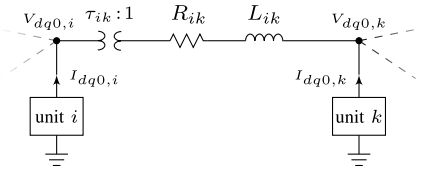

FIGURE 3. Single-line diagram of an *RL* transmission line connecting buses $i \to k$.

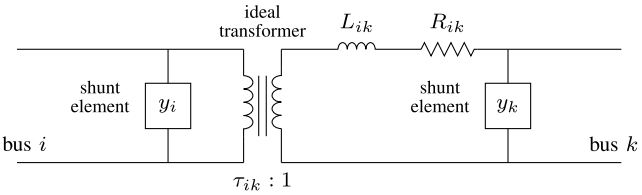

FIGURE 4. Standard branch connecting buses i and k.

To demonstrate this approach, consider a symmetric three-phase branch including a series connected transformer, resistor, and inductor, as depicted in Fig. 3. Combining equations (11), (14), and using the transformer ratio $\tau_{ik} : 1$, the dynamic equation representing the branch can be constructed in the state-space form as

$$\begin{aligned} \frac{\mathrm{d}}{\mathrm{d}t}I_{dq0,ik} = {} & \frac{1}{L_{ik}}\left(\frac{1}{\tau_{ik}}V_{dq0,i} - V_{dq0,k}\right) \\ & + \begin{bmatrix} -\frac{R_{ik}}{L_{ik}} & \omega_s & 0 \\ -\omega_s & -\frac{R_{ik}}{L_{ik}} & 0 \\ 0 & 0 & -\frac{R_{ik}}{L_{ik}} \end{bmatrix} I_{dq0,ik}. \end{aligned} \tag{17}$$

Hence, the current signals over the branch can be selected as states, and the outputs are defined according to Kirchhoff's current law. More sophisticated examples can be found in [45]. Similarly, the dynamic equations of a standard branch [39] as in Fig. 4 can be described as

$$\begin{aligned} \frac{\mathrm{d}}{\mathrm{d}t}\xi &= A_\xi \xi + B_\xi u \\ y &= C_\xi \xi + D_\xi u, \end{aligned} \tag{18}$$

where $u = [V_d, V_q, V_0]^{\mathsf{T}}$ and $y = [I_d, I_q, I_0]^{\mathsf{T}}$. The specific system matrices may be found in [38] and [46].

It was shown above that $dq0$ models can be directly obtained from abc models using (5). Now, we briefly review the similarities and differences between quasi-static and $dq0$ models and show that quasi-static models can be obtained from dq models at low frequencies. The traditional quasi-static model is based on the assumption that the frequency of voltage and current signals throughout the network is approximately constant. As a result, AC signals can be modeled accurately enough by means of time-varying phasors, and the transmission network can be described by a constant admittance matrix Y through the linear relation

$$I(t) = YV(t), \tag{19}$$

which is equivalent to the well-known power flow equations [47]. Equation (19) can alternatively be written in terms of its real and imaginary parts as

$$\begin{aligned} \mathrm{Re}\{I(t)\} &= \mathrm{Re}\{Y\}\,\mathrm{Re}\{V(t)\} - \mathrm{Im}\{Y\}\,\mathrm{Im}\{V(t)\}, \\ \mathrm{Im}\{I(t)\} &= \mathrm{Im}\{Y\}\,\mathrm{Re}\{V(t)\} + \mathrm{Re}\{Y\}\,\mathrm{Im}\{V(t)\}. \end{aligned} \tag{20}$$

Assume that the network is balanced. Then, a dynamic model based on dq signals is given by [16]

$$\begin{bmatrix} I_d(s) \\ I_q(s) \end{bmatrix} = \begin{bmatrix} \mathcal{N}_1(s) & j\mathcal{N}_2(s) \\ -j\mathcal{N}_2(s) & \mathcal{N}_1(s) \end{bmatrix} \begin{bmatrix} V_d(s) \\ V_q(s) \end{bmatrix}, \tag{21}$$

where

$$\begin{aligned} \mathcal{N}_1(s) &:= \frac{1}{2}\left(Y(s+j\omega_s) + Y(s-j\omega_s)\right), \\ \mathcal{N}_2(s) &:= \frac{1}{2}\left(Y(s+j\omega_s) - Y(s-j\omega_s)\right), \end{aligned} \tag{22}$$

and $Y(s)$ is the frequency dependent nodal admittance matrix. According to [8, Lemma 2], for $s = 0$, the dynamic model in (21) reduces to the quasi-static expressions in (20). This fact allows to realize quasi-static models as

$$\begin{bmatrix} I_d \\ I_q \end{bmatrix} = D_{qs} \begin{bmatrix} V_d \\ V_q \end{bmatrix} = \left(D_{dq} - C_{dq} A_{dq}^{-1} B_{dq}\right) \begin{bmatrix} V_d \\ V_q \end{bmatrix}, \tag{23}$$

where the system matrices are defined as in (18) with respect to the dq part.

Consider now a simple example of the balanced three-phase inductor. Starting from the quasi-static model, the admittance matrix describing the inductor is $Y = Y(j\omega_s) = 1/(j\omega_s L)$. Using time-varying phasors and (19), (20), the quasi-static model is given by

$$I = \frac{1}{j\omega_s L} V. \tag{24}$$

By taking the real and imaginary parts of this equation, and using the relations between dq signals and phasors $v_d = \sqrt{2}\,\mathrm{Re}\{V\}$, $v_q = \sqrt{2}\,\mathrm{Im}\{V\}$, equivalent expressions for the quasi-static model become

$$\begin{aligned} v_d &= -\omega_s L i_q, \\ v_q &= \omega_s L i_d. \end{aligned} \tag{25}$$

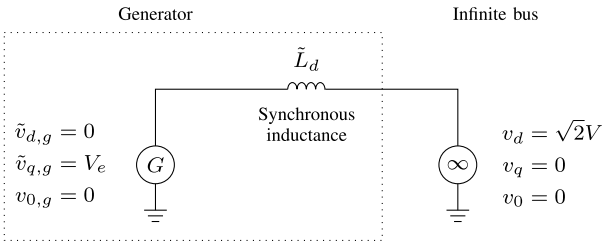

FIGURE 5. Single-phase diagram of a generator connected to an infinite bus.

In addition, recall that the dq model of the inductor (as in (11)) is given by

$$\begin{aligned} v_d &= -\omega_s L i_q + L\frac{\mathrm{d}}{\mathrm{d}t} i_d, \\ v_q &= \omega_s L i_d + L\frac{\mathrm{d}}{\mathrm{d}t} i_q. \end{aligned} \tag{26}$$

Direct comparison of these equations reveals that both models are similar, except for the additional time derivative terms in the dq model, which describe high-frequency effects. Note that at low-frequencies, where the time derivatives are negligible, both models are equivalent.

C. SYNCHRONOUS MACHINES

The $dq0$ transformation has been used over many years for modeling, analysis, and control of synchronous machines. There exist numerous books (e.g., [6], [28], [31], [48]–[52]) with detailed mathematical models of synchronous generators, excitation systems, and governing systems, based on $dq0$ quantities. To briefly demonstrate how the $dq0$ transformation is used for analyzing the dynamics of synchronous machines, the following discussion shows a model of a simple generator connected to an infinite bus. While such a model is popular in many textbooks, we recall here how to develop it based on the unified reference frame $\omega_s t$, instead of more traditional rotor angle θ. This is necessary for the model to be compatible with the network model, as discussed in Section III-B.

Consider a simple generator (with droop control mechanism) represented as an ideal voltage source behind an inductance $\tilde{L}_d$. The generator is connected to an infinite bus, as shown in Fig. 5. The generator voltage is $\tilde{v}_{d,g} = 0$, $\tilde{v}_{q,g} = V_e$, $v_{0,g} = 0$, with a reference angle of θ. In this example θ is the electric angle of the rotor in respect to the stator. The infinite bus has a constant frequency of ω_s, so its voltage is given by $v_d = V$, $v_q = 0$, $v_0 = 0$, with a reference angle of $\omega_s t$. Now the goal is to construct a dynamic model of the system based on $dq0$ signals. However, a potential problem is that the two voltage sources are defined with respect to two different reference frames (θ and $\omega_s t$). To solve this, we choose $\omega_s t$ as a unified reference frame for both the infinite bus and synchronous machine. The synchronous machine voltage is now obtained by substituting $\tilde{v}_{d,g} = 0$,

TABLE 2. Nomenclature: Synchronous machine.

λ_d, λ_q, λ_0	flux linkages
λ_f	field winding flux linkage
$\tilde{v}_d$, $\tilde{v}_q$, v_0	stator voltages
$\tilde{i}_d$, $\tilde{i}_q$, i_0	stator currents
v_f, i_f	field winding voltage and current
L_d, L_q, L_0	synchronous inductances
L_{af}	mutual inductance between the field winding and phase a
L_{ff}	self-inductance of the field winding
R_a, R_f	armature and field winding resistance
J	rotor moment of inertia
T_m	mechanical torque

$\tilde{v}_{q,g} = V_e$, $v_{0,g} = 0$ into (7), which leads to

$$\begin{aligned} v_{d,g} &= V_e \cos(\delta) \\ v_{q,g} &= V_e \sin(\delta) \\ v_{0,g} &= 0, \end{aligned} \tag{27}$$

and $\delta = \theta - \omega_s t + \pi/2$. Furthermore, the dynamic behavior of the angle δ is described by

$$\frac{\mathrm{d}^2}{\mathrm{d}t^2}\delta = \frac{\text{poles}}{2J\omega_s}\left(-P_{3\phi} + 3P_{ref} - \frac{1}{D}\frac{\mathrm{d}}{\mathrm{d}t}\delta\right), \tag{28}$$

which is the classic *swing equation* with the droop control mechanism. The term J is the rotor moment of inertia, *poles* is the number of machine poles (must be even), P_{ref} is the single-phase reference power, and D represents the droop control sloop parameter. The three-phase power can be computed by (8). Combination of (28) and (8) with $\delta = \phi_1$ results in the state equations

$$\begin{aligned} \frac{\mathrm{d}}{\mathrm{d}t}\delta &= \omega - \omega_s, \\ \frac{\mathrm{d}}{\mathrm{d}t}\omega &= \frac{\text{poles}}{2J\omega_s}\Big(-\frac{3}{2}V_e\left(\cos(\delta)i_d + \sin(\delta)i_q\right) \\ &\qquad + 3P_{ref} - \frac{1}{D}\left(\omega - \omega_s\right)\Big), \end{aligned} \tag{29}$$

and the outputs are defined by (27). Note that the model represents only the machine's voltage source, and does not include the synchronous inductance, which is represented separately in (11) with $L = \tilde{L}_d$.

For completeness, we now recall a more sophisticated (physical) model of a synchronous machine [28]. The model presented herein captures the interaction of the direct-axis magnetic field with the quadrature-axis mmf, and the quadrature-axis magnetic field with the direct-axis mmf, as well as the effects of resistances, transformer voltages, field winding dynamics, and salient poles. The parameters are explained in Table 2. Following [28], and omitting laborious algebraic manipulations, the resulting state equations of a synchronous machine in the $dq0$ reference frame (with respect to $\omega_s t$) are given by

$$\begin{aligned} \frac{\mathrm{d}}{\mathrm{d}t}\phi_1 &= -\frac{2R_aL_{ff}}{L_\beta^2}\phi_1 + \phi_2\phi_5 + \frac{2R_aL_{af}}{L_\beta^2}\phi_4 \\ &\quad + \sin(\phi_6)v_d - \cos(\phi_6)v_q, \\ \frac{\mathrm{d}}{\mathrm{d}t}\phi_2 &= -\frac{R_a}{L_q}\phi_2 - \phi_1\phi_5 + \cos(\phi_6)v_d + \sin(\phi_6)v_q, \\ \frac{\mathrm{d}}{\mathrm{d}t}\phi_3 &= -\frac{R_a}{L_0}\phi_3 + v_0, \\ \frac{\mathrm{d}}{\mathrm{d}t}\phi_4 &= \frac{3R_fL_{af}}{L_\beta^2}\phi_1 - \frac{2R_fL_d}{L_\beta^2}\phi_4 + v_f, \\ \frac{\mathrm{d}}{\mathrm{d}t}\phi_5 &= \frac{\text{poles}}{2J}\left(T_m + \frac{3L_\beta^2 - 6L_{ff}L_q}{2L_\beta^2L_q}\phi_1\phi_2 + \frac{3L_{af}}{L_\beta^2}\phi_2\phi_4\right), \\ \frac{\mathrm{d}}{\mathrm{d}t}\phi_6 &= \phi_5 - \omega_s, \end{aligned} \tag{30}$$

and the outputs are defined as

$$\begin{aligned} i_d &= -\frac{2L_{ff}}{L_\beta^2}\sin(\phi_6)\phi_1 - \frac{1}{L_q}\cos(\phi_6)\phi_2 + \frac{2L_{af}}{L_\beta^2}\sin(\phi_6)\phi_4, \\ i_q &= \frac{2L_{ff}}{L_\beta^2}\cos(\phi_6)\phi_1 - \frac{1}{L_q}\sin(\phi_6)\phi_2 - \frac{2L_{af}}{L_\beta^2}\cos(\phi_6)\phi_4, \\ i_0 &= -\frac{1}{L_0}\phi_3, \\ i_f &= -\frac{3L_{af}}{L_\beta^2}\phi_1 + \frac{2L_d}{L_\beta^2}\phi_4, \\ \omega &= \phi_5, \quad \delta = \phi_6, \end{aligned} \tag{31}$$

where $L_\beta^2 = 2L_dL_{ff} - 3L_{af}^2$. In this model, the state variables are selected as $\phi_1 = \lambda_d$, $\phi_2 = \lambda_q$, $\phi_3 = \lambda_0$, $\phi_4 = \lambda_f$, $\phi_5 = \omega$, $\delta = \phi_6$ and the inputs as v_d, v_q, v_0, v_f, T_m. Unlike the simplified model (29), this model already includes the inductance terms L_d, L_q, L_0. A convenient property of the model presented above is that its inputs and outputs are defined with respect to the unified reference frame rotating with $\omega_s t$, and therefore it can be directly connected to the network. For instance, connecting the synchronous machine model to an infinite bus is immediate by direct substitution of voltages v_d, v_q, v_0 from Fig. 5 into (30).

D. WIND ENERGY CONVERSION SYSTEMS

The dynamics of induction machines, which are typically used in wind energy conversion systems, are often studied in the $dq0$ reference frame. Induction machines can be categorized into two types: fixed and adjustable speed generators. Recently more attention is paid toward adjustable generators, and doubly-fed induction generators (DFIGs) in particular. The doubly-fed machines can be categorized into a standard or (single frame) cascaded doubly-fed induction machine and doubly-fed reluctance machine, see [53] for more detailed classification and comparison. Typical parameters of such machines are explained in Table 3, where subscripts d, q, s, r denote the dq components of the stator and rotor, respectively. Following [54], the resulting voltage

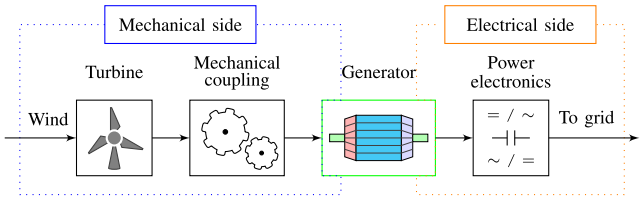

FIGURE 6. Block scheme of a typical wind turbine.

equations of a generator in the *dq* reference frame are given by

$$\begin{aligned} v_{d,s} &= R_s i_{d,s} + \frac{\mathrm{d}}{\mathrm{d}t}\phi_{d,s} - \omega_s \phi_{q,s} \\ v_{q,s} &= R_s i_{q,s} + \frac{\mathrm{d}}{\mathrm{d}t}\phi_{q,s} + \omega_s \phi_{d,s} \\ v_{d,r} &= R_r i_{d,r} + \frac{\mathrm{d}}{\mathrm{d}t}\phi_{d,r} - (\omega_s - \omega_r)\,\phi_{q,r} \\ v_{q,r} &= R_r i_{q,r} + \frac{\mathrm{d}}{\mathrm{d}t}\phi_{q,r} + (\omega_s - \omega_r)\,\phi_{d,r}, \end{aligned} \tag{32}$$

where ω_s is the nominal system frequency, ω_r denotes angular velocity of the rotor, and flux equations are represented as

$$\begin{aligned} \phi_{d,s} &= L_s i_{d,s} + L_{sr} i_{d,r} = \left(L_{l,s} + L_m\right) i_{d,s} + L_{sr} i_{d,r} \\ \phi_{q,s} &= L_s i_{q,s} + L_{sr} i_{q,r} = \left(L_{l,s} + L_m\right) i_{q,s} + L_{sr} i_{q,r} \\ \phi_{d,r} &= L_r i_{d,r} + L_{sr} i_{d,s} = \left(L_{l,r} + L_m\right) i_{d,r} + L_{sr} i_{d,s} \\ \phi_{q,r} &= L_r i_{q,r} + L_{sr} i_{q,s} = \left(L_{l,r} + L_m\right) i_{q,r} + L_{sr} i_{q,s}. \end{aligned} \tag{33}$$

In addition, the typical wind turbine system can be described by several principal components [55], [56], as shown in Fig. 6. Inclusion or exclusion of optional components depends on the specific application and generator type [57]. Detailed models based on the *dq*0 reference frame can be found in several overview papers. For example, work [58] gives an extensive overview of doubly-fed induction generators, and discusses their main advantages in comparison to other machines. In particular, several such advantages are variable speed operation, independent control of their active and reactive output powers, high energy efficiency, and low size. In addition, work [59] presents a general approach for modeling wind turbine systems, which is useful for power system dynamic simulations, and is compatible with existing software implementations. This paper follows the scheme presented in Fig. 6, but additionally discusses protection system and control of rotor and terminal voltage. Work [57] presents a literature overview on the different aspects of DFIGs. Specifically, the paper discusses various control methods used in wind turbine systems, including pitch angle control [60], vector and decoupling control [58], [61], [62], and passivity control methods [63], [64]. Finally, works [65]–[67] give an overview of the recent trends in standalone applications, as well as wind parks. These paper discuss specific grid connections, control issues, and perspectives of using particular types of generators.

TABLE 3. Nomenclature: Induction machine.

$v_{d,s}$, $v_{q,s}$, $v_{d,r}$, $v_{q,r}$	voltages
$i_{d,s}$, $i_{q,s}$, $i_{d,r}$, $i_{q,r}$	currents
$\phi_{d,s}$, $\phi_{q,s}$, $\phi_{d,r}$, $\phi_{q,r}$	fluxes
R_s, R_r	winding resistances
L_s, L_r	self-inductances
$L_{l,s}$, $L_{l,r}$	leakage inductances
L_{sr}	stator to rotor mutual inductance
L_m	magnetizing inductance

E. PHOTOVOLTAIC INVERTERS

The continuing growth of distributed generation is leading to networks with a mixture of classic rotating machines and inverter interfaced generators [68], among them photovoltaic inverters. Photovoltaic inverters are typically controlled either as *PQ* sources, in which case the active and reactive powers of the inverter are directly controlled, or as *PV* sources, where the active power and voltage amplitude are directly controlled [9], [69]–[72]. These two control schemes are associated with the two main operation modes for photovoltaic inverters, which are the grid-feeding [73], [74] and grid-forming modes [29], [75], [76]. Both control schemes can be implemented using lower level *dq*0-based controllers, as depicted in Fig. 7. As shown in a recent number of works, the *PQ* control scheme is more popular approach today, mainly since the output current of the inverter is well regulated, which enables robust and economically competitive designs. In many designs the reactive power is chosen to be zero, and the inverter is operated with a power factor of unity (for instance, as proposed in [77]). This approach leads to the lowest output current per active power, but the trade-off is that the inverter does not provide the reactive power that may be required to stabilize the grid.

A typical *PQ* control scheme is shown in Fig. 7(a). The design consists of an outer loop that controls the active power, and an inner current-control loop, which regulates the inverter output current. The outer loop regulates the active power in order to match it to the power produced by the photovoltaic source, where the feedback is provided by the bus-capacitor voltage. The active and reactive power set points are fed to the inner current controller, which regulates the output current using a *dq*0 reference frame rotating with the inverter output voltage. The reactive power set point may be chosen directly (for example, $Q^* = 0$), or may be manipulated to support a required voltage profile at the inverter output. More details may be found in [68]. It should be noted that this design omits many practical details, and is by no means the only design available.

Assume now that: *i*) high frequency switching harmonics are ignored; *ii*) the inverter is connected to the grid with a constant frequency ω_s; *iii*) all three-phase voltages and currents are balanced; *iv*) the PLL loop is ideal and perfectly extracts the *dq* components and frequency of the

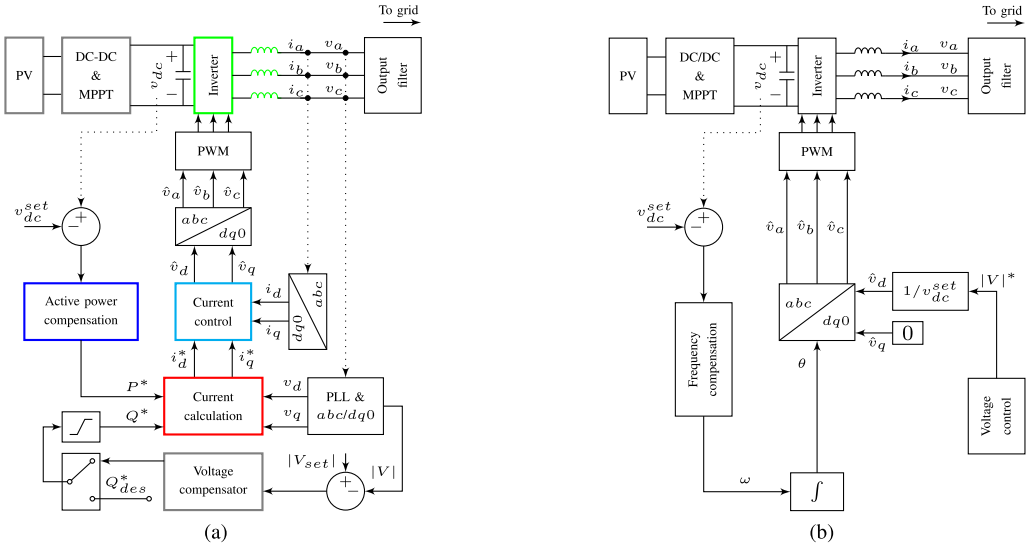

FIGURE 7. Typical control schemes of photovoltaic inverters based on *dq*0 quantities. (a) *PQ* control: active and reactive power. (b) *PV* control: active power and voltage.

grid voltage with zero distortion; *v*) the MPPT unit and DC-DC converter are ideal, and represented by a single constant power source (P_{dc}); *vi*) all power conversion stages are assumed to be ideal (lossless and no internal energy storage); *vii*) the current controller uses a common topology, as proposed in [68]. The current controller and active-power compensators are based on simple proportional-integral controllers. Then, the photovoltaic inverter based on *PQ* control scheme (Fig. 7(a)) can be described as follows. The main system components include:

✓ Active power control:

$$P^* = K_{p,p}\left(v_{dc} - v_{dc}^{set}\right) + z_1 + \frac{P_{dc}}{3} \tag{34}$$

such that

$$\begin{aligned}\frac{\mathrm{d}}{\mathrm{d}t}v_{dc} &= \frac{1}{v_{dc}^{set}C}\left(P_{dc} - P_{pv}\right),\\ \frac{\mathrm{d}}{\mathrm{d}t}z_1 &= K_{i,p}\left(v_{dc} - v_{dc}^{set}\right),\end{aligned} \tag{35}$$

and the output photovoltaic power is computed as

$$P_{pv} = \frac{3}{2}\left(\hat{v}_d i_d + \hat{v}_q i_q\right). \tag{36}$$

✓ Current calculation:

$$\begin{aligned}i_d^* &= \frac{2}{v_d^2 + v_q^2}\left(P^* v_d + Q^* v_q\right),\\ i_q^* &= \frac{2}{v_d^2 + v_q^2}\left(P^* v_q - Q^* v_d\right).\end{aligned} \tag{37}$$

✓ Current control:

$$\begin{aligned}\hat{v}_d &= v_d - \omega_s L i_q + K_{p,c}\left(i_d^* - i_d\right) + z_2,\\ \hat{v}_q &= v_q + \omega_s L i_d + K_{p,c}\left(i_q^* - i_q\right) + z_3,\end{aligned} \tag{38}$$

such that

$$\begin{aligned}\frac{\mathrm{d}}{\mathrm{d}t}z_2 &= K_{i,c}\left(i_d^* - i_d\right),\\ \frac{\mathrm{d}}{\mathrm{d}t}z_3 &= K_{i,c}\left(i_q^* - i_q\right).\end{aligned} \tag{39}$$

✓ Inverter and inductor (current injected to the grid):

$$\begin{aligned}\frac{\mathrm{d}}{\mathrm{d}t}i_d &= \frac{1}{L}\left(\hat{v}_d - v_d\right) + \omega_s i_q,\\ \frac{\mathrm{d}}{\mathrm{d}t}i_q &= \frac{1}{L}\left(\hat{v}_q - v_q\right) - \omega_s i_d.\end{aligned} \tag{40}$$

In the above equations C is the effective bus capacitor (transformed to bridge input), L is the total inductance (per phase) at the inverter output, v_{dc}^{set} is the desired bus voltage (transformed to bridge input), P_{dc} is the inverter DC input power at steady-state (equals to the total three-phase output power), and $K_{p,p}$, $K_{i,p}$, $K_{p,c}$, $K_{i,c}$ are parameters of the PI controllers. In addition, the inputs (from the grid) are v_d, v_q, P_{dc}, and the outputs (to the grid) are i_d, i_q.

F. PHASE-LOCKED LOOPS

In many practical applications an essential part of the control circuitry is a Phase-Locked Loop (PLL), which senses the three-phase voltages and estimates their associated phase and *dq* components. A basic PLL design is shown in Fig. 8, which is adopted from [68]. The main ideas are briefly summarized as follows. The loop operates by controlling the angle θ of the *dq* transformation such that *q*-axis component is zeroed. This is achieved by a negative feedback loop, in which the loop compensator acts to zero its input while maintaining stability. In Fig. 8 the signals are defined as: $\widetilde{V}_{dq0}$ is the mathematical transformation of the real *a*, *b*, *c* signals, using a reference frame rotating with θ_c. The angle θ_c is predetermined and well-defined. In addition, V_{dq0} denotes estimated signals,

TABLE 4. DQ0 transformation: Summary of application areas.

Unit	Model type	Refs.
Transmission networks	transient	[2], [9], [16], [36]–[38]
Microgrids	transient	[9], [41], [42], [44]
	small-signal	[43]
Synchronous machines	transient	[6], [28], [31], [48]–[52], [100], [101]
	small-signal	[6], [37]
Wind turbines	transient	[53]–[64], [66], [102]–[108]
	small-signal	[109]
Photovoltaic inverters	transient	[9], [29], [68]–[77], [110]–[113]
PLL	transient	[68], [78]–[94], [96]–[99], [114]
	small-signal	[93], [95]
Rectifiers	transient	[115]–[119]
	small-signal	[120]–[124]

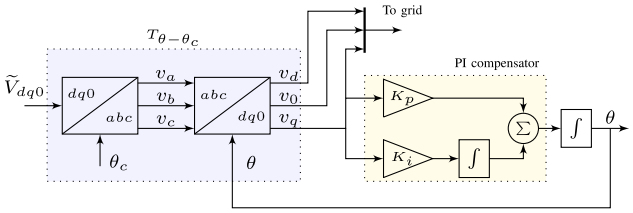

FIGURE 8. Basic model of a conventional PLL based on *dq*0 signals.

defined with respect to a reference frame θ, such that $v_q = 0$ at steady-state. To avoid transformation to the *abc* reference frame and keep the signals in terms of *dq*0 quantities, one can define (similar to (7)) a new transformation as

$$\begin{bmatrix} v_d \\ v_q \\ v_0 \end{bmatrix} = \underbrace{\begin{bmatrix} \cos(\theta-\theta_c) & \sin(\theta-\theta_c) & 0 \\ -\sin(\theta-\theta_c) & \cos(\theta-\theta_c) & 0 \\ 0 & 0 & 1 \end{bmatrix}}_{T_{\theta-\theta_c}} \begin{bmatrix} \tilde{v}_d \\ \tilde{v}_q \\ v_0 \end{bmatrix}. \tag{41}$$

Furthermore, the PI compensator can be described as

$$\begin{aligned} \dot{\phi} &= K_i v_q, \\ \dot{\theta} &= K_p v_q + \phi. \end{aligned} \tag{42}$$

Equations (41) and (42) together constitute the *dq*0 model of a basic PLL system.

PLLs are usually required when there is a need to synchronize a unit to the grid (e.g., inverters) and also for monitoring and control purposes. A comprehensive review of recent PLL schemes is presented in [78]. Recent challenges in this area include

- exploring ways to realize/implement PLLs of different types [79]–[82];
- seeking methods to improve the dynamic performance of PLLs using, for example, adaptive frequency estimation loop [83] or adaptive loop gain [84];
- improving the filtering capability and disturbance rejection ability of PLLs by including different filters inside their control loop or before their input such as:
  - moving average filter [85];
  - notch filter [86], [87];
  - multiple synchronous reference frame filtering [88], [89];
  - complex-coefficient-filter [90], [91];
  - delayed signal cancellation [92]–[96];
  - second-order generalized integrator [94], [97].

Finally, it was recently noticed that the droop control and PLLs structurally resemble each other [98], [99]. This relation creates additional possibilities for future research, which can improve and further develop both techniques.

IV. DISCUSSION AND CONCLUSION

With increasing penetration of distributed and renewable sources into power grids, and with increasing use of power electronics based devices, the dynamic behavior of large-scale power systems are becoming increasingly complex. Several systematic issues are:

- Active power balancing
- Reactive power balancing
- Reduced system inertia
- Fast transients
- Stability issues, due to interactions between power electronics based components
- Frequency regulation issues due to increasing integration of power electronics generators
- Resonance due to interactions between power electronics based devices and power lines
- Poor damping of local and inter-area oscillations.

Stability and dynamic responses of large-scale power systems are often studied by means of time-varying phasors, under the assumption that the system is quasi-static. However, with increasing integration of fast renewable and distributed sources, this assumption is becoming increasingly inaccurate. In this light, the *dq*0 transformation provides several

important advantages that simplify the system dynamics, especially when modeling balanced or symmetrically configured power systems. One advantage is that sinusoidal three phase signals are mapped to constant signals at steady-state, so *dq*0-based models have a well-defined operating point, and therefore enable small-signal and stability analysis. In addition, *dq*0 models capture the actual behavior of networks and devices, and are accurate at high frequencies. Models based on the *dq*0 transformation also allow a formal extension of quasi-static (time-varying phasor) models to high frequencies, without assuming a quasi-static system, and without sacrificing accuracy.

A current challenge is to merge various *dq*0 based models appearing in the literature to allow modeling of large-scale power systems. In light of this challenge, this paper provides an overview of recent *dq*0 models of the network and its main components. We explain basic concepts related to the *dq*0 transformation and *dq*0-based models, and review several recent models of passive components, networks, synchronous machines, photovoltaic inverters, wind turbines, rectifiers, and others. A central objective of this review is to promote *dq*0-based analysis not only of single machines, but also of large-scale power systems. This in turn may allow a better understanding of the dynamics associated with the integration of distributed and renewable energy sources.

REFERENCES

[1] P. Kundur, "Definition and classification of power system stability IEEE/CIGRE joint task force on stability terms and definitions," *IEEE Trans. Power Syst.*, vol. 19, no. 3, pp. 1387–1401, May 2004.

[2] M. Ilić and J. Zaborszky, *Dynamics and Control of Large Electric Power Systems*. New York, NY, USA: Wiley, 2000.

[3] P. C. Stefanov and A. M. Stanković, "Modeling of UPFC operation under unbalanced conditions with dynamic phasors," *IEEE Trans. Power Syst.*, vol. 17, no. 2, pp. 395–403, May 2002.

[4] Y. Liu, K. Sun, and Y. Liu, "A measurement-based power system model for dynamic response estimation and instability warning," *Electr. Power Syst. Res.*, vol. 124, pp. 1–9, Jul. 2015.

[5] L. Miller, L. Cibulka, M. Brown, and A. von Meier, "Electric distribution system models for renewable integration: Status and research gaps analysis," California Energy Commission, Sacramento, CA, USA, Tech. Rep. CEC-500-10-055, Jul. 2013.

[6] P. M. Anderson and A. A. Fouad, *Power System Control and Stability*. Hoboken, NJ, USA: Wiley, 2008.

[7] R. Yousefian and S. Kamalasadan, "A Lyapunov function based optimal hybrid power system controller for improved transient stability," *Electr. Power Syst. Res.*, vol. 137, pp. 6–15, Aug. 2016.

[8] J. Belikov and Y. Levron, "Comparison of time-varying phasor and dq0 dynamic models for large transmission networks," *Int. J. Elect. Power Energy Syst.*, vol. 93, pp. 65–74, Dec. 2017.

[9] J. Schiffer, D. Zonetti, R. Ortega, A. M. Stanković, T. Sezi, and J. Raisch, "A survey on modeling of microgrids—From fundamental physics to phasors and voltage sources," *Automatica*, vol. 74, pp. 135–150, Dec. 2016.

[10] S. Almer and U. Jonsson, "Dynamic phasor analysis of periodic systems," *IEEE Trans. Autom. Control*, vol. 54, no. 8, pp. 2007–2012, Aug. 2009.

[11] A. M. Stanković, S. R. Sanders, and T. Aydin, "Dynamic phasors in modeling and analysis of unbalanced polyphase AC machines," *IEEE Trans. Energy Convers.*, vol. 17, no. 1, pp. 107–113, Mar. 2002.

[12] M. Daryabak *et al.*, "Modeling of LCC-HVDC systems using dynamic phasors," *IEEE Trans. Power Del.*, vol. 29, no. 4, pp. 1989–1998, Aug. 2014.

[13] T. Demiray, G. Andersson, and L. Busarello, "Evaluation study for the simulation of power system transients using dynamic phasor models," in *Proc. Transmiss. Distrib. Conf. Expo.*, Bogotá, Colombia, Aug. 2008, pp. 1–6.

[14] T. Demiray and G. Andersson, "Comparison of the efficiency of dynamic phasor models derived from ABC and DQO reference frame in power system dynamic simulations," in *Proc. 7th IET Int. Conf. Adv. Power Syst. Control, Oper. Manage.*, Hong Kong, Oct./Nov. 2006, pp. 1–8.

[15] T. Yang, S. V. Bozhko, and G. M. Asher, "Modeling of uncontrolled rectifiers using dynamic phasors," in *Proc. Elect. Syst. Aircraft, Railway Ship Propuls.*, Oct. 2012, pp. 1–6.

[16] Y. Levron and J. Belikov, "Modeling power networks using dynamic phasors in the *dq*0 reference frame," *Electr. Power Syst. Res.*, vol. 144, pp. 233–242, Mar. 2017.

[17] A. M. Stanković and T. Aydin, "Analysis of asymmetrical faults in power systems using dynamic phasors," *IEEE Trans. Power Syst.*, vol. 15, no. 3, pp. 1062–1068, Aug. 2000.

[18] C. Liu, A. Bose, and P. Tian, "Modeling and analysis of HVDC converter by three-phase dynamic phasor," *IEEE Trans. Power Del.*, vol. 29, no. 1, pp. 3–12, Feb. 2014.

[19] H. Zhu, Z. Cai, H. Liu, Q. Qi, and Y. Ni, "Hybrid-model transient stability simulation using dynamic phasors based HVDC system model," *Electr. Power Syst. Res.*, vol. 76, nos. 6–7, pp. 582–591, Apr. 2006.

[20] M. C. Chudasama and A. M. Kulkarni, "Dynamic phasor analysis of SSR mitigation schemes based on passive phase imbalance," *IEEE Trans. Power Syst.*, vol. 26, no. 3, pp. 1668–1676, Aug. 2011.

[21] Z. Miao, L. Piyasinghe, J. Khazaei, and L. Fan, "Dynamic phasor-based modeling of unbalanced radial distribution systems," *IEEE Trans. Power Syst.*, vol. 30, no. 6, pp. 3102–3109, Nov. 2015.

[22] S. Chandrasekar and R. Gokaraju, "Dynamic phasor modeling of type 3 DFIG wind generators (including SSCI phenomenon) for short-circuit calculations," *IEEE Trans. Power Del.*, vol. 30, no. 2, pp. 887–897, Apr. 2015.

[23] T. Bi, H. Liu, Q. Feng, C. Qian, and Y. Liu, "Dynamic phasor model-based synchrophasor estimation algorithm for M-class PMU," *IEEE Trans. Power Del.*, vol. 30, no. 3, pp. 1162–1171, Jun. 2015.

[24] D. G. Lee, S. H. Kang, and S. R. Nam, "Modified dynamic phasor estimation algorithm for the transient signals of distributed generators," *IEEE Trans. Smart Grid*, vol. 4, no. 1, pp. 419–424, Mar. 2013.

[25] R. K. Mai, L. Fu, Z. Y. Dong, K. P. Wong, Z. Q. Bo, and H. B. Xu, "Dynamic phasor and frequency estimators considering decaying DC components," *IEEE Trans. Power Syst.*, vol. 27, no. 2, pp. 671–681, May 2012.

[26] T. Yang, S. Bozhko, J. M. Le-Peuvedic, G. Asher, and C. I. Hill, "Dynamic phasor modeling of multi-generator variable frequency electrical power systems," *IEEE Trans. Power Syst.*, vol. 31, no. 1, pp. 563–571, Jan. 2016.

[27] X. Guo, Z. Lu, B. Wang, X. Sun, L. Wang, and J. M. Guerrero, "Dynamic phasors-based modeling and stability analysis of droop-controlled inverters for microgrid applications," *IEEE Trans. Smart Grid*, vol. 5, no. 6, pp. 2980–2987, Nov. 2014.

[28] A. E. Fitzgerald, C. Kingsley, Jr., and S. D. Umans, *Electric Machinery*, 6th ed. New York, NY, USA: McGraw-Hill, 2003.

[29] R. Teodorescu, M. Liserre, and P. Rodriguez, *Grid Converters for Photovoltaic and Wind Power Systems*. Hoboken, NJ, USA: Wiley, 2011.

[30] R. H. Park, "Two-reaction theory of synchronous machines generalized method of analysis—Part I," *Trans. Amer. Inst. Electr. Eng.*, vol. 48, no. 3, pp. 716–727, Jul. 1929.

[31] P. C. Krause, O. Wasynczuk, S. D. Sudhoff, and S. Pekarek, *Analysis of Electric Machinery and Drive Systems*, 3rd ed. Hoboken, NJ, USA: Wiley, 2013.

[32] P. W. Sauer and M. A. Pai, *Power System Dynamics and Stability*. Upper Saddle River, NJ, USA: Prentice-Hall, 1998.

[33] C. T. Rim, D. Y. Hu, and G. H. Cho, "Transformers as equivalent circuits for switches: General proofs and D-Q transformation-based analyses," *IEEE Trans. Ind. Appl.*, vol. 26, no. 4, pp. 777–785, Jul./Aug. 1990.

[34] W. H. Kwon and G. H. Cho, "Analyses of static and dynamic characteristics of practical step-up nine-switch matrix convertor," *IEE Proc. B-Electr. Power Appl.*, vol. 140, no. 2, pp. 139–146, Mar. 1993.

[35] P. Szcześniak, Z. Fedyczak, and M. Klytta, "Modelling and analysis of a matrix-reactance frequency converter based on buck-boost topology by DQ0 transformation," in *Proc. 13th Int. Power Electron. Motion Control Conf.*, Sep. 2008, pp. 165–172.

[36] P. W. Sauer, B. C. Lesieutre, and M. A. Pai, "Transient algebraic circuits for power system dynamic modelling," *Int. J. Elect. Power Energy Syst.*, vol. 15, no. 5, pp. 315–321, Jan. 1993.

[37] Y. Levron and J. Belikov, "Observable canonical forms of multi-machine power systems using dq0 signals," in *Proc. IEEE Int. Conf. Sci. Elect. Eng.*, Eilat, Israel, Nov. 2016, pp. 1–6.

[38] J. Belikov and Y. Levron, "A sparse minimal-order dynamic model of power networks based on dq0 signals," *IEEE Trans. Power Syst.*, to be published, doi: 10.1109/TPWRS.2017.2702746.

[39] R. D. Zimmerman, C. E. Murillo-Sánchez, and R. J. Thomas, "MATPOWER: Steady-state operations, planning, and analysis tools for power systems research and education," *IEEE Trans. Power Syst.*, vol. 26, no. 1, pp. 12–19, Feb. 2011.

[40] F. Katiraei, M. R. Iravani, and P. W. Lehn, "Small-signal dynamic model of a micro-grid including conventional and electronically interfaced distributed resources," *IET Generat., Transmiss. Distrib.*, vol. 1, no. 3, pp. 369–378, May 2007.

[41] M. Babazadeh and H. Karimi, "Robust decentralized control for islanded operation of a microgrid," in *Proc. Power Energy Soc. Gen. Meet.*, Detroit, MI, USA, Jul. 2011, pp. 1–8.

[42] M. S. Mahmoud, S. A. Hussain, and M. A. Abido, "Modeling and control of microgrid: An overview," *J. Franklin Inst.*, vol. 351, no. 5, pp. 2822–2859, 2014.

[43] M. Rasheduzzaman, J. A. Mueller, and J. W. Kimball, "An accurate small-signal model of inverter-dominated islanded microgrids using *dq* reference frame," *IEEE J. Emerg. Sel. Topics Power Electron.*, vol. 2, no. 4, pp. 1070–1080, Dec. 2014.

[44] Y. Ojo and J. Schiffer, "Towards a time-domain modeling framework for small-signal analysis of unbalanced microgrids," in *Proc. 12th IEEE PES PowerTech Conf.*, Manchester, U.K., Jun. 2017, pp. 1–6.

[45] J. Belikov and Y. Levron, "Integration of long transmission lines in large-scale dq0 dynamic models," *Elect. Eng.*, to be published, doi: 10.1007/s00202-017-0582-7.

[46] Y. Levron and J. Belikov. (2017). DQ0 dynamics—Software manual. Technion—Israel Institute of Technology, Haifa, Israel. [Online]. Available: http://a-lab.ee/sites/default/files/manual.pdf

[47] J. J. Grainger and W. D. Stevenson, Jr., *Power System Analysis*. New York, NY, USA: McGraw-Hill, 1994.

[48] P. Kundur, *Power System Stability and Control*. New York, NY, USA: McGraw-Hill, 1994.

[49] T. Wildi, *Electrical Machines, Drives and Power Systems*, 5th ed. Upper Saddle River, NJ, USA: Pearson Education, 2002.

[50] X.-F. Wang, Y. Song, and M. Irving, "Mathematical model of synchronous generator and load," in *Modern Power Systems Analysis*. Boston, MA, USA: Springer, 2008, pp. 333–404.

[51] S. J. Chapman, *Electric Machinery Fundamentals*, 5th ed. Blacklick, OH, USA: McGraw-Hill, 2011.

[52] J. Machowski, J. Bialek, and J. Bumby, *Power System Dynamics: Stability and Control*. Hoboken, NJ, USA: Wiley, 2011.

[53] B. Hopfensperger and D. J. Atkinson, "Doubly-fed a.c. machines: Classification and comparison," in *Proc. Eur. Conf. Power Electron. Appl.*, Graz, Austria, 2001, pp. 27–29.

[54] Q. Chen, Y. Li, and J. E. Seem, "Dual-loop self-optimizing robust control of wind power generation with doubly-fed induction generator," *ISA Trans.*, vol. 58, pp. 409–420, 2015.

[55] Z. Chen and F. Blaabjerg, "Wind energy: The world's fastest growing energy source," *IEEE Power Electron. Soc. Newslett.*, vol. 18, no. 3, pp. 15–19, Sep. 2006.

[56] J. G. Njiri and D. Söffker, "State-of-the-art in wind turbine control: Trends and challenges," *Renew. Sust. Energ. Rev.*, vol. 60, pp. 377–393, Jul. 2016.

[57] M. Tazil *et al.*, "Three-phase doubly fed induction generators: An overview," *IET Electr. Power Appl.*, vol. 4, no. 2, pp. 75–89, 2010.

[58] S. Müller, M. Deicke, and R. W. De Doncker, "Doubly fed induction generator systems for wind turbines," *IEEE Ind. Appl. Mag.*, vol. 8, no. 3, pp. 26–33, May/Jun. 2002.

[59] J. G. Slootweg, S. W. H. D. Haan, H. Polinder, and W. L. Kling, "General model for representing variable speed wind turbines in power system dynamics simulations," *IEEE Trans. Power Syst.*, vol. 18, no. 1, pp. 144–151, Feb. 2003.

[60] S. Heier, *Grid Integration of Wind Energy: Onshore and Offshore Conversion Systems*. Chichester, U.K.: Wiley, 2014.

[61] R. Pena, J. C. Clare, and G. M. Asher, "Doubly fed induction generator using back-to-back PWM converters and its application to variable-speed wind-energy generation," *IEE Proc.-Electr. Power Appl.*, vol. 143, no. 3, pp. 231–241, May 1996.

[62] H. Huang, Y. Fan, R.-C. Qiu, and X.-D. Jiang, "Quasi-steady-state rotor EMF-oriented vector control of doubly fed winding induction generators for wind-energy generation," *Electr. Power Compon. Syst.*, vol. 34, no. 11, pp. 1201–1211, 2006.

[63] S. Lee and K. Nam, "Dynamic modelling and passivity-based control of an induction motor powered by doubly fed induction generator," in *Proc. Ind. Appl. Conf., 38th IAS Annu. Meet.*, Salt Lake City, UT, USA, Oct. 2003, pp. 1970–1975.

[64] S. Aissi, L. Saidi, and A. Rachid, "Passivity based control of doubly fed induction machine using a fuzzy controller," *Int. J. Adv. Sci. Technol.*, vol. 36, pp. 51–64, Nov. 2011.

[65] J. M. Carrasco *et al.*, "Power-electronic systems for the grid integration of renewable energy sources: A survey," *IEEE Trans. Ind. Electron.*, vol. 53, no. 4, pp. 1002–1016, Jun. 2006.

[66] M. Liserre, R. Cárdenas, M. Molinas, and J. Rodríguez, "Overview of multi-MW wind turbines and wind parks," *IEEE Trans. Ind. Electron.*, vol. 58, no. 4, pp. 1081–1095, Apr. 2011.

[67] Y. Kumar *et al.*, "Wind energy: Trends and enabling technologies," *Renew. Sustain. Energy Rev.*, vol. 53, pp. 209–224, Jan. 2016.

[68] N. Kroutikova, C. A. Hernandez-Aramburo, and T. C. Green, "State-space model of grid-connected inverters under current control mode," *IET Electr. Power Appl.*, vol. 1, no. 3, pp. 329–338, May 2007.

[69] J. A. P. Lopes, C. L. Moreira, and A. G. Madureira, "Defining control strategies for microgrids islanded operation," *IEEE Trans. Power Syst.*, vol. 21, no. 2, pp. 916–924, May 2006.

[70] J. Rocabert, A. Luna, F. Blaabjerg, and P. Rodríguez, "Control of power converters in AC microgrids," *IEEE Trans. Power Electron.*, vol. 27, no. 11, pp. 4734–4749, Nov. 2012.

[71] X. Wang, J. M. Guerrero, F. Blaabjerg, and Z. Chen, "A review of power electronics based microgrids," *J. Power Electron.*, vol. 12, no. 1, pp. 181–192, 2012.

[72] S. Adhikari, F. Li, and H. Li, "P-Q and P-V control of photovoltaic generators in distribution systems," *IEEE Trans. Smart Grid*, vol. 6, no. 6, pp. 2929–2941, Nov. 2015.

[73] F. Katiraei, R. Iravani, N. Hatziargyriou, and A. Dimeas, "Microgrids management," *IEEE Power Energy Mag.*, vol. 6, no. 3, pp. 54–65, May/Jun. 2008.

[74] S. Bolognani and S. Zampieri, "A distributed control strategy for reactive power compensation in smart microgrids," *IEEE Trans. Autom. Control*, vol. 58, no. 11, pp. 2818–2833, Nov. 2013.

[75] P. C. Loh and D. G. Holmes, "Analysis of multiloop control strategies for LC/CL/LCL-filtered voltage-source and current-source inverters," *IEEE Trans. Ind. Appl.*, vol. 41, no. 2, pp. 644–654, Mar. 2005.

[76] N. Pogaku, M. Prodanovic, and T. C. Green, "Modeling, analysis and testing of autonomous operation of an inverter-based microgrid," *IEEE Trans. Power Electron.*, vol. 22, no. 2, pp. 613–625, Mar. 2007.

[77] M. F. Schonardie, R. F. Coelho, R. Schweitzer, and D. C. Martins, "Control of the active and reactive power using dq0 transformation in a three-phase grid-connected PV system," in *Proc. IEEE Int. Symp. Ind. Electron.*, May 2012, pp. 264–269.

[78] S. Golestan, J. M. Guerrero, and J. C. Vasquez, "Three-phase PLLs: A review of recent advances," *IEEE Trans. Power Electron.*, vol. 32, no. 3, pp. 1894–1907, Mar. 2017.

[79] H. Geng, D. Xu, and B. Wu, "A novel hardware-based all-digital phase-locked loop applied to grid-connected power converters," *IEEE Trans. Ind. Electron.*, vol. 58, no. 5, pp. 1737–1745, May 2011.

[80] S. Golestan, M. Monfared, F. D. Freijedo, and J. M. Guerrero, "Advantages and challenges of a type-3 PLL," *IEEE Trans. Power Electron.*, vol. 28, no. 11, pp. 4985–4997, Nov. 2013.

[81] S. Golestan, F. D. Freijedo, A. Vidal, J. M. Guerrero, and J. Doval-Gandoy, "A quasi-type-1 phase-locked loop structure," *IEEE Trans. Power Electron.*, vol. 29, no. 12, pp. 6264–6270, Dec. 2014.

[82] C. Subramanian and R. Kanagaraj, "Rapid tracking of grid variables using prefiltered synchronous reference frame PLL," *IEEE Trans. Instrum. Meas.*, vol. 64, no. 7, pp. 1826–1836, Jul. 2015.

[83] M. K. Ghartemani, S. Khajehoddin, P. K. Jain, and A. Bakhshai, "Problems of startup and phase jumps in PLL systems," *IEEE Trans. Power Electron.*, vol. 27, no. 4, pp. 1830–1838, Apr. 2012.

[84] T. Thacker, D. Boroyevich, R. Burgos, and F. Wang, "Phase-locked loop noise reduction via phase detector implementation for single-phase systems," *IEEE Trans. Ind. Electron.*, vol. 58, no. 6, pp. 2482–2490, Jun. 2011.
[85] S. Golestan, M. Ramezani, J. M. Guerrero, F. D. Freijedo, and M. Monfared, "Moving average filter based phase-locked loops: Performance analysis and design guidelines," *IEEE Trans. Power Electron.*, vol. 29, no. 6, pp. 2750–2763, Jun. 2014.
[86] F. D. Freijedo, J. Doval-Gandoy, O. Lopez, and E. Acha, "Tuning of phase-locked loops for power converters under distorted utility conditions," *IEEE Trans. Ind. Appl.*, vol. 45, no. 6, pp. 2039–2047, Nov./Dec. 2009.
[87] F. Gonzalez-Espin, G. Garcerá, I. Patrao, and E. Figueres, "An adaptive control system for three-phase photovoltaic inverters working in a polluted and variable frequency electric grid," *IEEE Trans. Power Electron.*, vol. 27, no. 10, pp. 4248–4261, Oct. 2012.
[88] L. Hadjidemetriou, E. Kyriakides, and F. Blaabjerg, "A new hybrid PLL for interconnecting renewable energy systems to the grid," *IEEE Trans. Ind. Appl.*, vol. 49, no. 6, pp. 2709–2719, Nov./Dec. 2013.
[89] S. Golestan, M. Monfared, and F. D. Freijedo, "Design-oriented study of advanced synchronous reference frame phase-locked loops," *IEEE Trans. Power Electron.*, vol. 28, no. 2, pp. 765–778, Feb. 2013.
[90] X. Guo, W. Wu, and Z. Chen, "Multiple-complex coefficient-filter-based phase-locked loop and synchronization technique for three-phase grid-interfaced converters in distributed utility networks," *IEEE Trans. Ind. Electron.*, vol. 58, no. 4, pp. 1194–1204, Apr. 2011.
[91] S. Golestan, M. Monfared, F. D. Freijedo, and J. M. Guerrero, "Performance improvement of a prefiltered synchronous-reference-frame PLL by using a PID-type loop filter," *IEEE Trans. Ind. Electron.*, vol. 61, no. 7, pp. 3469–3479, Jul. 2014.
[92] Y. F. Wang and Y. W. Li, "Three-phase cascaded delayed signal cancellation PLL for fast selective harmonic detection," *IEEE Trans. Ind. Electron.*, vol. 60, no. 4, pp. 1452–1463, Apr. 2013.
[93] S. Golestan, M. Ramezani, J. M. Guerrero, and M. Monfared, "dq-frame cascaded delayed signal cancellation-based PLL: Analysis, design, and comparison with moving average filter-based PLL," *IEEE Trans. Power Electron.*, vol. 30, no. 3, pp. 1618–1632, Mar. 2015.
[94] M. Xie, H. Wen, C. Zhu, and Y. Yang, "DC offset rejection improvement in single-phase SOGI-PLL algorithms: Methods review and experimental evaluation," *IEEE Access*, vol. 5, pp. 12810–12819, 2017.
[95] H. A. Hamed, A. F. Abdou, E. H. E. Bayoumi, and E. E. El-Kholy, "Frequency adaptive CDSC-PLL using axis drift control under adverse grid condition," *IEEE Trans. Ind. Electron.*, vol. 64, no. 4, pp. 2671–2682, Apr. 2017.
[96] S. Golestan, J. M. Guerrero, and J. C. Vasquez, "Hybrid adaptive/nonadaptive delayed signal cancellation-based phase-locked loop," *IEEE Trans. Ind. Electron.*, vol. 64, no. 1, pp. 470–479, Jan. 2017.
[97] Z. Xin, X. Wang, Z. Qin, M. Lu, P. C. Loh, and F. Blaabjerg, "An improved second-order generalized integrator based quadrature signal generator," *IEEE Trans. Power Electron.*, vol. 31, no. 12, pp. 8068–8073, Dec. 2016.
[98] Q.-C. Zhong and D. Boroyevich, "Structural resemblance between droop controllers and phase-locked loops," *IEEE Access*, vol. 4, pp. 5733–5741, 2016.
[99] Q.-C. Zhong, "Power-electronics-enabled autonomous power systems: Architecture and technical routes," *IEEE Trans. Ind. Electron.*, vol. 64, no. 7, pp. 5907–5918, Jul. 2017.
[100] B. A. Welchko, T. M. Jahns, and S. Hiti, "IPM synchronous machine drive response to a single-phase open circuit fault," *IEEE Trans. Power Electron.*, vol. 17, no. 5, pp. 764–771, Sep. 2002.
[101] M. Fasil, C. Antaloae, N. Mijatovic, B. B. Jensen, and J. Holboll, "Improved *dq*-axes model of PMSM considering airgap flux harmonics and saturation," *IEEE Trans. Appl. Supercond.*, vol. 26, no. 4, Jun. 2016, Art. no. 5202705.
[102] A. Medina and R. Cisneros, "Power quality assessment with a state space model of a wind park in dq0 coordinates," in *Proc. Elect. Power Energy Conf.*, Montreal, QC, Canada, Oct. 2009, pp. 1–6.
[103] J. Martínez and A. Medina, "A state space model for the dynamic operation representation of small-scale wind-photovoltaic hybrid systems," *Renew. Energy*, vol. 35, no. 6, pp. 1159–1168, 2010.
[104] F. D. Kanellos, G. J. Tsekouras, and N. D. Hatziargyriou, "Wind parks equivalent ARX models for the simulation of power systems with large wind power penetration, using system-identification theory," *Electr. Power Syst. Res.*, vol. 81, no. 2, pp. 707–715, 2011.
[105] J. Tamura, "Calculation method of losses and efficiency of wind generators," in *Wind Energy Conversion Systems*, S. M. Muyeen, Ed. London, U.K.: Springer-Verlag, 2012, pp. 25–51.
[106] M. Zamanifar, B. Fani, M. E. H. Golshan, and H. R. Karshenas, "Dynamic modeling and optimal control of DFIG wind energy systems using DFT and NSGA-II," *Electr. Power Syst. Res.*, vol. 108, pp. 50–58, Mar. 2014.
[107] H. Li, C. Yang, Y. Hu, X. Liao, Z. Zeng, and C. Zhe, "An improved reduced-order model of an electric pitch drive system for wind turbine control system design and simulation," *Renew. Energy*, vol. 93, pp. 188–200, Aug. 2016.
[108] A. Jafari and G. Shahgholian, "Analysis and simulation of a sliding mode controller for mechanical part of a doubly-fed induction generator-based wind turbine," *IET Generat., Transmiss. Distrib.*, vol. 11, no. 10, pp. 2677–2688, 2017.
[109] H. Liu, X. Xie, Y. Li, H. Liu, and Y. Hu, "A small-signal impedance method for analyzing the SSR of series-compensated DFIG-based wind farms," in *Proc. Power Energy Soc. Gen. Meet.*, Denver, CO, USA, Jul. 2015, pp. 1–5.
[110] A. Bonfiglio, M. Brignone, F. Delfino, and R. Procopio, "Optimal control and operation of grid-connected photovoltaic production units for voltage support in medium-voltage networks," *IEEE Trans. Sustain. Energy*, vol. 5, no. 1, pp. 254–263, Jan. 2014.
[111] C. Buccella, C. Cecati, H. Latafat, and K. Razi, "Multi string grid-connected PV system with LLC resonant DC/DC converter," *Intell. Ind. Syst.*, vol. 1, no. 1, pp. 37–49, 2015.
[112] M. D. Ilić, "Toward a unified modeling and control for sustainable and resilient electric energy systems," *Found. Trends Electr. Energy Syst.*, vol. 1, nos. 1–2, pp. 1–141, 2016.
[113] M. D. Ilić, R. Jaddivada, and X. Miao, "Modeling and analysis methods for assessing stability of microgrid," in *Proc. 20th IFAC World Congr.*, Toulouse, France, Jul. 2017.
[114] X. Wang, L. Harnefors, and F. Blaabjerg, "A unified impedance model of grid-connected voltage-source converters," *IEEE Trans. Power Electron.*, to be published, doi: 10.1109/TPEL.2017.2684906.
[115] R. Crosier and S. Wang, "DQ-frame modeling of an active power filter integrated with a grid-connected, multifunctional electric vehicle charging station," *IEEE Trans. Power Electron.*, vol. 28, no. 12, pp. 5702–5716, Dec. 2013.
[116] Q. Lei, S. Liang, F. Z. Peng, M. Shen, and V. Blasko, "A generalized DQ impedance model of three phase diode rectifier," in *Proc. IEEE Energy Convers. Congr. Expo.*, Denver, CO, USA, Sep. 2013, pp. 3340–3347.
[117] S. Kumar, N. Kumaresan, M. Subbiah, and M. Rageeru, "Modelling, analysis and control of stand-alone self-excited induction generator-pulse width modulation rectifier systems feeding constant DC voltage applications," *IET Generat., Transmiss. Distrib.*, vol. 8, no. 6, pp. 1140–1155, Jun. 2014.
[118] T. Gao and J. Zhao, "Dynamic model for VIENNA rectifier operating in continuous and discontinuous conduction mode," in *Proc. 41st Annu. Conf. IEEE Ind. Electron. Soc.*, Yokohama, Japan, Nov. 2015, pp. 000977–000982.
[119] M. Hamouda, H. F. Blanchette, and K. Al-Haddad, "Unity power factor operation of indirect matrix converter tied to unbalanced grid," *IEEE Trans. Power Electron.*, vol. 31, no. 2, pp. 1095–1107, Feb. 2016.
[120] S.-B. Han, N.-S. Choi, C.-T. Rim, and G.-H. Cho, "Modeling and analysis of static and dynamic characteristics for buck-type three-phase PWM rectifier by circuit DQ transformation," *IEEE Trans. Power Electron.*, vol. 13, no. 2, pp. 323–336, Mar. 1998.
[121] X. J. Yang, W. Cai, P. S. Ye, and Y. M. Gong, "Research on dynamic characteristics of matrix rectifier," in *Proc. Conf. Ind. Electron. Appl.*, Singapore, May 2006, pp. 1–6.
[122] K.-N. Areerak, S. V. Bozhko, G. M. Asher, and D. W. P. Thomas, "Stability analysis and modelling of AC-DC system with mixed load using DQ-transformation method," in *Proc. Int. Symp. Ind. Electron.*, Cambridge, U.K., Jun./Jul. 2008, pp. 19–24.
[123] K. Chaijarurnudomrung, K.-N. Areerak, and K.-L. Areerak, "Modeling of three-phase controlled rectifier using a DQ method," in *Proc. Int. Conf. Adv. Energy Eng.*, Beijing, China, Jun. 2010, pp. 56–59.
[124] C. Wan, M. Huang, C. K. Tse, and X. Ruan, "Effects of interaction of power converters coupled via power grid: A design-oriented study," *IEEE Trans. Power Electron.*, vol. 30, no. 7, pp. 3589–3600, Jul. 2015.

DMITRY BAIMEL received the B.S. degree from the Shamoon College of Engineering, Israel, in 2004, and the M.S. and Ph.D. degrees in electrical engineering from the Ben-Gurion University of the Negev, Israel, in 2008 and 2013, respectively. He is currently a Senior Lecturer with the Shamoon College of Engineering. His research interests include power systems, renewable energy, and smart grids.

JURI BELIKOV received the B.S. degree in mathematics from Tallinn University in 2006, and the M.S. and Ph.D. degrees in computer and systems engineering from the Tallinn University of Technology in 2008 and 2012, respectively. From 2015 to 2017, he was a Post-Doctoral Fellow with the Faculty of Mechanical Engineering and the Andrew and Erna Viterbi Faculty of Electrical Engineering, Technion—Israel Institute of Technology, Haifa, Israel. He is currently an Associate Professor with the Department of Computer Systems, Tallinn University of Technology, Tallinn, Estonia. His main research interests lie in the domains of nonlinear control theory and power systems.

JOSEP M. GUERRERO (S'01–M'04–SM'08–F'15) received the B.S. degree in telecommunications engineering, the M.S. degree in electronics engineering, and the Ph.D. degree in power electronics from the Technical University of Catalonia, Barcelona, Spain, in 1997, 2000, and 2003, respectively. Since 2011, he has been a Full Professor with the Department of Energy Technology, Aalborg University, Aalborg, Denmark, where he is responsible for the Microgrid Research Program. Since 2012, he has been a Guest Professor with the Chinese Academy of Science and the Nanjing University of Aeronautics and Astronautics; and since 2014, he has been a Chair Professor with Shandong University.

His research interests are oriented to different microgrid aspects, including power electronics, distributed energy-storage systems, hierarchical and cooperative control, energy management systems, and the optimization of microgrids and islanded minigrids. In 2015, he became a fellow of the IEEE for contributions to distributed power systems and microgrids. He was awarded by Thomson Reuters as an ISI Highly Cited Researcher.

YOASH LEVRON (M'13) received the B.S. degree (*summa cum laude*) in electrical engineering from the Technion—Israel Institute of Technology, Haifa, Israel, in 2001, and the M.S. and Ph.D. degrees in electrical engineering from Tel-Aviv University in 2007 and 2013, respectively. From 2013 to 2014, he was a Post-Doctoral Fellow with the Colorado Power Electronics Center, University of Colorado at Boulder, Boulder, CO, USA. He is currently an Assistant Professor with the Department of Electrical Engineering, Technion—Israel Institute of Technology. He has received several awards, including the group award of Israel Security in 2008 and 2010, the Technion Viterbi Fellowship for nurturing future faculty members (2013–2014), and the Taub Fellowship for leaders in science and technology (2015).